EPJ Web of Conferences **117**, 03002 (2016) DOI: 10.1051/epjconf/201611703002
NN2015

An overview of resonance measurements at the ALICE experiment

A. G. Knospe (for the ALICE Collaboration)

The University of Texas at Austin, Austin, TX, USA

Abstract

Resonances play a unique role in the study of ultra-relativistic heavy-ion collisions. Resonance yields, which may be modified by rescattering and regeneration after hadronization, can be used to study the properties of the hadronic phase of the collision. The transverse-momentum spectra of the proton and the $\phi(1020)$ can be used to study the mechanisms of particle production. In addition, resonance measurements in pp and p–Pb collisions help to distinguish initial-state effects from the effects of the hot and dense final state. The ALICE Collaboration has studied the $K^*(892)^0$ and $\phi(1020)$ mesons in pp, p–Pb, and Pb–Pb collisions. Measurements of many resonance properties, including p_T spectra, integrated yields, masses, widths, mean p_T values, and the nuclear modification factors R_{AA} and R_{pPb}, are presented and compared to measurements from other experiments, non-resonances, and the predictions of theoretical models.

In relativistic heavy-ion collisions, strongly interacting matter is studied under extreme conditions. Based on quantum chromodynamics (QCD), it is expected that when hadronic matter reaches a high enough energy density a transition will occur in which quarks become deconfined [1–3]. In this state of matter, the quark-gluon plasma (QGP), the relevant degrees of freedom are not hadrons, but rather quarks and gluons. For low baryochemical potentials (typical of heavy-ion collisions at the LHC), the transition between hadronic matter and the QGP is expected to occur around a temperature of $T_c \approx 160$ MeV [3–5]. Experimentally, this is achieved by colliding nuclei at

very high energies (a center-of-mass energy per nucleon-nucleon pair, $\sqrt{s_{\rm NN}}$, greater than a few tens of GeV). An ultra-relativistic heavy-ion collision is expected to produce a QGP, which thermalizes, expands, and cools for a few fm/c before making the transition back to hadronic matter. The hadronic system continues to expand and cool. It first passes chemical freeze-out, after which inelastic interactions cease and the yield of (most) particle species are fixed. Elastic interactions continue until kinetic freeze-out, after which the system is too diffuse to interact. Typical estimates of the time between chemical and kinetic freeze-out are ~ 10 fm/c [6, 7].

These proceedings focus on the use of hadronic resonances as probes of heavy-ion collisions. In addition to deconfinement, strongly interacting matter is expected to undergo a transition in which chiral symmetry is restored and the quark masses approach 0. Lattice QCD calculations [8] suggest that the deconfinement and chiral transitions occur around the same temperature. Resonances that decay when chiral symmetry was (partially) restored may exhibit shifted masses or increased widths [9–12].

The yields of stable particles are expected to be fixed at chemical freeze-out, but the measured yields of resonances, which can decay during the hadronic phase, may be changed by scattering processes involving their decay products [13–15]. Resonance yields can be regenerated when hadrons undergo pseudo-elastic scattering through a resonance state. Experimentally, resonances are reconstructed in invariant-mass analyses; if one of the resonance decay products undergoes elastic scattering in the hadronic medium, the resonance invariant-mass peak may be smeared out, reducing the reconstructible resonance yield. The decay product of one resonance may also undergo pseudo-elastic scattering through a different resonance state, removing information about the original resonance and reducing its measured yield [6]. The strengths of these processes depend on the chemical freeze-out temperature, the time between chemical and kinetic freeze-out, the lifetime of the resonance, and the scattering cross sections of its decay products. Regeneration and re-scattering are expected to be most important for $p_{\rm T} \lesssim 2$ GeV/c [6, 13].

In addition, resonances can be used along with stable particles to study the properties of the collision system and their effects on hadrons with different flavors, masses, and baryon numbers. Specifically, resonances can be used to study partonic energy loss in the deconfined system, which is quantified using the nuclear modification factor (discussed below). They can also be used to study the mechanisms through which particles are produced and the effects that modify the shapes of particle $p_{\rm T}$ spectra (see, in particular, the discussion of the p/ϕ(1020) ratio below).

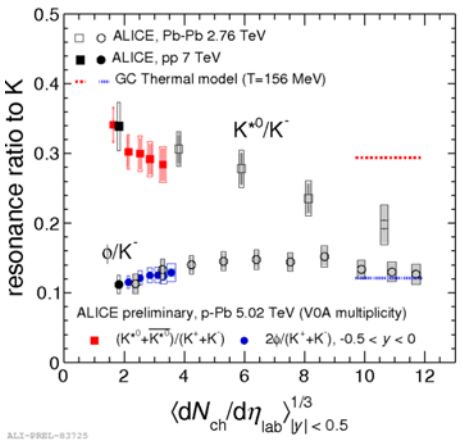

Figure 1: K^{*0}/K^{-} and ϕ/K^{-} ratios as a function of the mid-rapidity $\langle dN_{ch}/d\eta \rangle^{1/3}$ for pp, p–Pb, and Pb–Pb collisions [16–18]. Bars represent statistical uncertainties, open boxes represent total systematic uncertainties, and shaded boxes represent the parts of the systematic uncertainties that are uncorrelated between multiplicity or centrality intervals.

These proceedings focus on measurements by the ALICE Collaboration of the $K^*(892)^0$ and $\overline{K}^*(892)^0$ resonances (sum or average denoted as K^{*0}), as well as the $\phi(1020)$ meson (denoted by ϕ). These resonances are reconstructed via their decay to charged hadrons: $K^{*0} \rightarrow \pi^{\pm}K^{\mp}$ (branching ratio 0.667) and $\phi \rightarrow K^{-}K^{+}$ (branching ratio 0.489). For a description of the technique, see [16, 17].

The ALICE Collaboration has measured the masses and widths of the K^{*0} and ϕ mesons by reconstructing their decays in Pb–Pb collisions at $\sqrt{s_{NN}} = 2.76$ TeV [17]. The measured masses and widths of these particles are consistent with their vacuum values. The lack of the expected signatures of chiral symmetry restoration may be due to the loss of resonances produced early in the collision due to re-scattering and the regeneration of additional resonances late in the collision.

Figure 1 shows the p_T-integrated K^{*0}/K and ϕ/K ratios measured in pp, p–Pb, and Pb–Pb collisions at LHC energies [16–18]. These ratios are plotted as funcitons of $\langle dN_{ch}/d\eta \rangle^{1/3}$ (measured at mid-rapidity: $|\eta| < 0.5$), which is taken as a proxy for the system size. The K^{*0}/K ratio is significantly suppressed in central Pb–Pb collision with respect to smaller collision systems (pp collisions at $\sqrt{s} = 7$ TeV and p–Pb collisions at $\sqrt{s_{NN}} = 5.02$ TeV). (A "central" collision is one with a small impact paramter, in which the volume of the system is largest; a "peripheral" collision has a large impact parameter and smaller system size.) This suppression may be due to signal loss resulting from re-scattering of the K^{*0} decay products in the hadronic medium (which would be dominant over regeneration). In contrast, the ϕ/K ratio depends only weakly on system size and is not suppressed in central Pb–Pb collisions, suggesting that the longer-lived ϕ meson is affected less

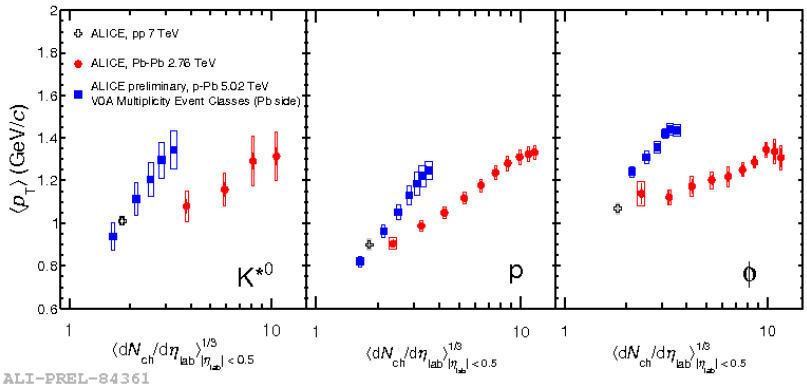

Figure 2: Measurements of $\langle p_{\mathrm{T}} \rangle$ of K^{*0}, p, and ϕ in pp, p–Pb, and Pb–Pb collisions [18]. Bars (boxes) represent statistical (systematic) uncertainties.

by re-scattering in the hadronic phase. For both ratios, the values measured in p–Pb collisions are similar to the values measured in pp and Pb–Pb collision with similar multiplicities. These ratios are also compared to the values given by a thermal-model fit to particle yields measured by ALICE in central Pb–Pb collisions with a chemical freeze-out temperature of 156 MeV (the fit includes the ϕ yield, but not the K^{*0}). The K^{*0}/K ratio is suppressed with respect to the thermal-model value, while the ϕ is not supressed. As described in [17], the measured K^{*0}/K ratio in central Pb–Pb collisions can be compared to an extended thermal model (modified to include re-scattering effects) [14, 19, 20] to extract a model-dependent estimate of the time between chemical and kinetic freeze-out. When this is done, a lower limit of 2 fm/c is found (only a lower limit can be extracted because the model does not include regeneration).

The K^{*0} and ϕ mesons can also be used along with other particles in studies of how flavor, mass, and baryon number affect the shapes of particle p_{T} spectra, which can be characterized using the mean transverse momentum $\langle p_{\mathrm{T}} \rangle$. Figure 2 shows the $\langle p_{\mathrm{T}} \rangle$ of three particles with similar masses, K^{*0}, p, and ϕ, measured in pp, p–Pb, and Pb–Pb collisions [18]. In central Pb–Pb collisions, the $\langle p_{\mathrm{T}} \rangle$ values of these three particles are consistent with each other. Hydrodynamic models have been found to provide good descriptions of the matter produced in heavy-ion collisions [21–23]. In such models, the particle mass tends to be the dominant factor in determining the shape of the p_{T} spectrum; the similarity of the $\langle p_{\mathrm{T}} \rangle$ values for K^{*0}, p, and ϕ therefore appears to be consistent with what would be expected from hydrodynamic models. In contrast, in smaller collision systems (pp, p–Pb, and peripheral

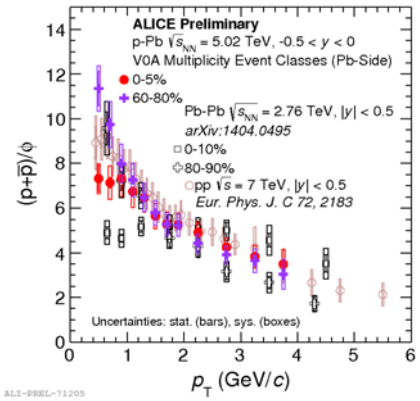

Figure 3: Ratio p/ϕ as a function of p_{T} for p, and ϕ in pp, p–Pb, and Pb–Pb collisions. Bars (boxes) represent statistical (systematic) uncertainties.

Pb–Pb collisions) a splitting is observed between the $\langle p_{\mathrm{T}} \rangle$ values of p and ϕ, suggesting that factors other than the particle mass are playing important roles in determining the shapes of the p_{T} spectra. It should also be noted that (unlike the K^{*0}/K and ϕ/K ratios) the $\langle p_{\mathrm{T}} \rangle$ values in p–Pb collisions follow different trends than observed in Pb–Pb collisions. The $\langle p_{\mathrm{T}} \rangle$ values for K^{*0}, p, and ϕ rise much faster as functions of $\langle \mathrm{d}N_{\mathrm{ch}}/\mathrm{d}\eta \rangle^{1/3}$ in Pb–Pb collisions and reach (or even exceed) the values observed in central Pb–Pb collisions, despite the very different system sizes.

When central Pb–Pb collisions are compared to pp collisions, an enhancement is observed in p_{T}-dependent baryon-to-meson ratios such as p/π and Λ/K^0_S [24, 25] for $1.5 \lesssim p_{\mathrm{T}} \lesssim 6$ GeV/c at RHIC and LHC energies. Various explanations have been proposed to explain this enhancement. In a hydrodynamic picture the enhancement can be explained by the difference in the particle masses: all particles would have a common flow velocity, so more massive particles would be pushed out to higher p_{T}, resulting in an enhancement in their ratios to less massive particles (see, for example, [21–23]). In recombination models [26, 27], the quark content and the number of valence (anti)quarks may play a role in determining the shapes of particle p_{T} spectra. Such models might therefore yield different shapes for the p_{T} spectra of baryons and mesons (even those with similar masses). Since the (anti)proton and ϕ have similar masses, their ratio can be used to study this effect, as shown in fig. 3 [18]. The p/ϕ ratio is constant as a function of p_{T} for central Pb–Pb collisions at $\sqrt{s_{\mathrm{NN}}} = 2.76$ TeV, while developing a slope for more peripheral collision (as well as for p–Pb and pp collisions; not shown). The constant ratio in central collisions is consistent with a hydrodynamic interpretation, but it should be noted that some recombination models can also reproduce the observed behavior [28].

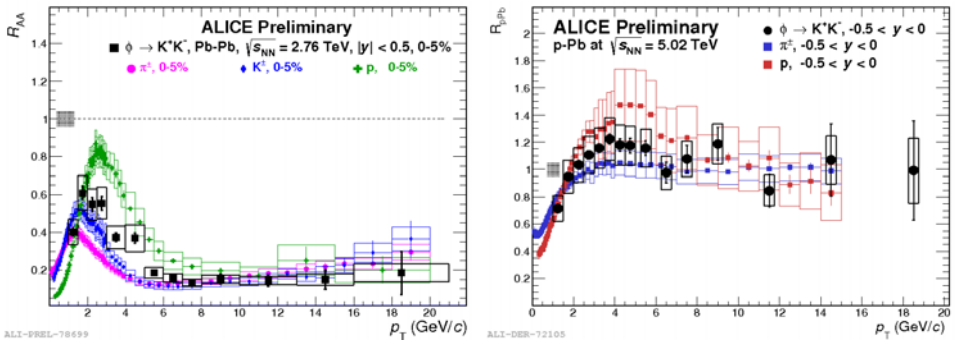

Figure 4: Nuclear modification factors R_{AA} (left) and R_{pPb} (right) of various hadrons. Bars (boxes) represent statistical (systematic) uncertainties.

It is also possible to use the ϕ meson along with other particles in studies of the flavor, mass, and baryon-number dependence of parton energy loss in the QGP. The effect of nuclear matter R_{AA} on particle yields is quantified using the nuclear modification factor: the ratio of the yield in A–A collisions to the same yield in pp collisions scaled by the number of binary nucleon-nucleon collisions in the A–A coillison. If the A–A collision is a simple superposition of NN collisions, R_{AA} would be unity. Figure 4 (left) shows R_{AA} as a function of p_{T} for the ϕ meson and for light hadrons; the suppression at intermediate and high p_{T} is attributed to parton energy loss in the QGP. The high-p_{T} suppression is the same for almost all hadron species (including those containing c and b quarks). For $2 < p_{\mathrm{T}} < 6$ GeV/c, there appears to be mass ordering in the R_{AA} values for mesons. At RHIC, different shapes for R_{AA} of (anti)protons and ϕ was taken as evidence in favor of recombination models, but in the present data the different R_{AA} values for these particles are due to differences in the reference (pp) spectra. Figure 4 (right) shows R_{pPb}, the nuclear modification factor for p–Pb collisions, which quantifies the effect of nuclear matter in the absence of a QGP (so-called "cold nuclear matter"). The R_{pPb} for $\pi^{\pm}$ is consistent with unity for $p_{\mathrm{T}} > 2.5$ GeV/c, while R_{pPb} for protons exhibits a moderate enhancement. The R_{pPb} values for ϕ are consistent with unity for intermediate and high p_{T}, though there are hints of a small Cronin enhancement. Taken together, these R_{AA} and R_{pPb} suggest the presence of mass dependence and/or baryon/meson differences for the processes that determine the shapes of particle spectra in pp, p–Pb, and Pb–Pb collisions.

Hadronic resonances are useful probes in the study of heavy-ion collisions. Their short lifetimes make them well suited to study the properties

of the hadronic phase. They can also be compared to other particles as part of systematic studies of the flavor, mass, and baryon-number dependence of the process that determine the shapes of particle p_{T} spectra. The ALICE Collaboration has measured the K^{*0} and ϕ mesons in multiple collision systems [16–18] and has also measured the $\Sigma(1385)^{\pm}$ and $\Xi(1530)^{0}$ baryonic resonances in pp collisions [29]. There are also ongoing measurements of several particles, including $\rho(770)^{0}$, Σ^{0}, $\Delta(1232)^{++}$, $\Sigma(1385)^{\pm}$, $\Lambda(1520)$, and $\Xi(1530)^{0}$ in pp, p–Pb, and Pb–Pb collisions at LHC energies. The p_{T}-integrated $\mathrm{K}^{*0}/\mathrm{K}$ ratio is observed to be suppressed in central Pb–Pb collisions, consistent with signal loss due to re-scattering of the K^{*0} decay products, while the longer-lived ϕ meson is not suppressed. Measurements of $\langle p_{\mathrm{T}} \rangle$ and the p_{T}-dependent p/ϕ ratio indicate that hydrodynamics (in which particle masses are a dominant factor in determining the shapes of p_{T} spectra) is well suited to describe central Pb–Pb collisions, while effects depending on quark content may be important for smaller collision systems. As quantified by the nuclear modification factor R_{AA}, particle suppression at high p_{T} is the same for most particle species; at intermediate p_{T} there may be mass and/or baryon-number dependence.

References

[1] Petreczky P., *Proc. of Science (Confinement X)* (2012) 028.

[2] Borsányi S. *et al.*, *J. High Energy Phys.*, **11** (2010) 077.

[3] Borsányi S. *et al.*, *J. High Energy Phys.*, **09** (2010) 073.

[4] Aoki Y. *et al.*, *J. High Energy Phys.*, **06** (2009) 088.

[5] Bazavov A. *et al.*, *Phys. Rev.* D, **85** (2012) 054503.

[6] Bleicher M. and Aichelin J., *Phys. Lett.* B, **530** (2002) 81–87.

[7] Bass S. A. *et al.*, *Phys. Rev.* C, **60** (1999) 021902.

[8] Petreczky P., *Nucl. Phys.* A, **785** (2007) 10–17.

[9] Brown G. E. and Rho M., *Rhys. Rep.*, **363** (2002) 85–171.

[10] Rapp R. *et al.*, *Relativistic Heavy Ion Physics*, edited by Stock R., (Springer Berlin Heidelberg) 2010, pp. 134–175.

[11] Brodsky S. J. and de Teramond G. F., *Phys. Rev. Lett.*, **60** (1988) 1924.

[12] Eletsky V. L. *et al.*, *Phys. Rev.* C, **64** (2001) 035202.

[13] Bleicher M. and Stöcker H., *J. Phys.* G, **30** (2004) S111–S118.

[14] Markert C. *et al.*, *AIP Conf. Proc.*, **631** (2002) 533-552.

[15] Vogel S. and Bleicher M., *Ricerca Scientifica ed Educazione Permanente*, edited by I. Iori and A. Bortolotti, Supplemento N. 124 (Università degli Studi di Milano, Milan) 2005, pp. 116–119, nucl-th/0505027 Preprint.

[16] Abelev B. *et al.* (ALICE Collaboration), *Eur. Phys. J.* C, **72** (2012) 2183.

[17] Abelev B. *et al.* (ALICE Collaboration), *Phys. Rev.* C, **91** (2015) 024609.

[18] Bellini F. (for the ALICE Collaboration), *Nucl. Phys.* A, **931** (2014) 846–850.

[19] Torrieri G. and Rafelski J., *Phys. Lett.* B, **509** (2001) 239–245.

[20] Rafelski J. *et al.*, *Phys. Rev.* C, **64** (2001) 054907.

[21] Qui Z. *et al.*, *Phys. Lett.* B, **707** (2012) 151–155.

[22] Shen C. *et al.*, *Phys. Rev.* C, **84** (2011) 044903.

[23] Bożek P. and Wyskiel-Piekarska I., *Phys. Rev.* C, **85** (2012) 064915.

[24] Abelev B. *et al.* (ALICE Collaboration), *Phys. Rev.* C, **88** (2013) 044910.

[25] Abelev B. *et al.* (ALICE Collaboration), *Phys. Rev. Lett.*, **111** (2013) 222301.

[26] Fries R. *et al.*, *Phys. Rev. Lett.*, **90** (2003) 202303.

[27] Fries R. *et al.*, *Annu. Rev. Nucl. Part. Sci*, **58** (2008) 177–205.

[28] Minissale V. *et al.*, *Phys. Rev.* C, **92** (2015) 054904.

[29] Abelev B. *et al.* (ALICE Collaboration), *Eur. Phys. J.* C, **75** (2015) 1.